Carbohydrate Polymers 113 (2014) 264–271

Contents lists available at ScienceDirect

Carbohydrate Polymers

journal homepage: www.elsevier.com/locate/carbpol

Flexible, highly transparent and iridescent all-cellulose hybrid nanopaper with enhanced mechanical strength and writable surface

Rui Xiong, Yangyang Han, Yaru Wang, Wei Zhang, Xinxing Zhang*, Canhui Lu*

State Key Laboratory of Polymer Materials Engineering, Polymer Research Institute of Sichuan University, Chengdu 610065, China

ARTICLE INFO

Article history:
Received 25 March 2014
Received in revised form 19 May 2014
Accepted 25 June 2014
Available online 17 July 2014

Keywords:
Cellulose nanofibrils
Cellulose nanowhiskers
Transparent nanopaper
Flexible electronics

ABSTRACT

With the development of flexible electronic devices, there is increasing requirement for the inexpensive and environmental-friendly substrates. Cellulose paper has gained great attention because of its abundance, biodegradability and renewability. In this paper, we designed a hybrid nanopaper by introducing native cellulose nanofibrils (CNFs) into cellulose nanowhiskers (CNWs) matrix, which achieved a high optical transmittance while retaining iridescence under polarizing film. This nanopaper is less expensive than neat CNFs-based nanopaper and more feasible for large-scale production. Besides, our transparent hybrid nanopaper possesses the writable surface like regular paper. Compared with commercial paper, however, hybrid nanopaper shows superior optical properties and low surface roughness. The combination of these characteristics makes this nanopaper an excellent candidate for substrates of flexible electronic devices.

1. Introduction

Cellulose, known as the most abundant natural polymer on earth, has become an important renewable chemical resource to replace petroleum-based materials (Beck, Bouchard, & Berry, 2011; Ma, Zhou, Li, Li, & Ou, 2011). Wood cellulose fiber has been used for more than thousands years as an ingredient for making paper, which is a widely used material in everyday life. As it is renewable, environment friendly, scalable, light weight, mechanically flexible and disposable, cellulose paper is recently being explored as a promising sustainable substrate for use in electronic devices (Fang et al., 2011; Gao et al., 2013). Various electronic devices such as displays (Madaria, Kumar, & Zhou, 2011), transistors (Russo et al., 2011), batteries (Nyholm, Nyström, Mihranyan, & Strømme, 2011) and solar cells (Hu & Cui, 2012) have been reported to be printed on regular paper. However, regular paper is made of cellulose fibers with a diameter in the range of 20–50 mm, which results in a series of shortcomings such as the large surface roughness, porous structure, and optical opaqueness to hosting electronic devices on the surface of this material (Zhu et al., 2013).

Recently, considerable interest has been directed to cellulose nanofibrils (CNFs) since they are well known that cellulose nanofibers have a coefficient of thermal expansion (CTE) of 0.1 ppm/K and an estimated strength of 2–3 GPa (Guo, Chen, & Yan, 2013). Besides, CNFs are virtually free from light scattering, which makes it possible to prepare optically transparent nanopaper with strong tensile strength, a low CTE and a low surface roughness (Zhu et al., 2013). Reports on nanopaper and its applications have arisen in recent years, mainly focusing on engineered nanostructures of cellulose to fabricate transparent and flexible electronic devices, such as nanopaper organic light-emitting diodes (Zhang, Zhang, Lu, Wang, & Deng, 2012), conductive transparent paper (Jung et al., 2008), magnetic nanopaper (Li et al., 2013) and nanopaper lithium-ion batteries (Hu et al., 2013). However, it is a costly process to extract CNFs from wood fibers as it requires high energy consumption, expensive equipment, time-consuming procedure and low yield rate. Recently, in order to reduce the cost of nanopaper, Fang et al. (Fang et al., 2013) have prepared a kind of all-cellulose hybrid nanostructured paper with a writable surface, which has a superior smoothness and high optical transmittance.

Cellulose nanowhiskers (CNWs), another form of nanocellulose, are generated by removing the amorphous sections of purified cellulose source through acid hydrolysis (Klemm et al., 2011). CNWs consists of rod-like cellulose crystals with widths of 5–70 nm and lengths of 100–1000 nm (Xiong, Zhang, Tian, Zhou, & Lu, 2012). Under a certain condition, CNWs can self-assemble into an anisotropic chiral nematic liquid crystalline phase (Klemm et al., 2011). Comparing with the CNFs, the cost of CNWs is much lower since the preparation procedure is facile and time-saving and does not need the expensive professional mechanical equipment. Owing to the absence of amorphous sections, however, CNWs film is so fragile that it needs other nanofillers to enhance their mechanical

* Corresponding authors. Tel.: +86 28 85460607; fax: +86 28 85402465.
E-mail addresses: xxzwwh@scu.edu.cn (X. Zhang), canhuilu@scu.edu.cn (C. Lu).

http://dx.doi.org/10.1016/j.carbpol.2014.06.069
0144-8617/

properties (especially flexibility). As a new class of nanoreinforcement in green nanocomposites, CNFs has attracted great attention because of its unique characteristics such as high aspect ratio and good mechanical properties (Chen, Yu, Li, Liu, & Li, 2011a; Chen et al., 2011b; Chen, Yu, & Liu, 2011c). Therefore, it would be very interesting to combine the two kinds of nanocellulose materials.

In this manuscript, we demonstrate a flexible, highly optical transparent and iridescent CNFs/CNWs hybrid nanopaper that possesses a writable surface for flexible electronics. Furthermore, it is iridescent under polarizing film and less expensive than that of neat CNWs-based nanopaper. In our hybrid paper, CNFs was used as a nanoreinforcement to be incorporated into CNWs paper, which aims to improve the mechanical properties of iridescent CNWs paper and thus facilitate their applications. CNFs fills the spaces to decrease the light scattering that otherwise occurs in CNWs paper substrates. Compared with CNWs nanopaper, hybrid paper has a greater optical transparency and mechanical strength.

2. Materials and methods

2.1. Preparation of CNWs suspension

The CNWs suspension was obtained by acid hydrolysis of commercial cotton. About 5 g of commercial cotton was dispersed in 100 mL of sulfuric acid (64 wt%) at 45 °C under vigorous stirring for 60 min. The suspensions were then washed with deionized water using repeatedly centrifuge cycles (10 min at 12,000 rpm for a cycle) until the suspension reached neutrality. Finally, the samples were ultrasonic treated for 10 min in an ice bath. The resulted CNWs suspension was concentrated to 1.59 wt% by evaporation.

2.2. Preparation of CNFs suspension

Never-dried bamboo bleached fibers were used as cellulose source for preparing CNFs. The method to prepare CNFs is according to Chen et al. (Chen et al., 2011a, 2011b, 2011c). 100 mL solution containing purified cellulose fibers (0.1 wt%) was ultrasonically treated for 200 min with a common ultrasonic generator (JY99-II D, Ningbo Scientz Biotechnology Co., Ltd., China) at a frequency of 19.5–20.5 kHz. Then the upper CNFs suspension was collected.

2.3. Preparation of hybrid nanopaper

The mixed suspension containing different ratios of CNWs and CNFs was prepared by homogenization using a high shear mixer (IKA T18). This mixed suspension was filled into a diameter petri dish (90 mm) and allowed to evaporate over 48 h at ambient temperature to produce hybrid nanopaper. The thickness of each nanopaper was kept constantly at 50 ± 10 μm. The samples were coded as nanopaper-0, nanopaper-1, nanopaper-5, and nanopaper-10, according to the solid content of CNFs in the nanopapers at 0 wt%, 1 wt%, 5 wt%, and 10 wt%, respectively.

2.4. Characterization

2.4.1. Measurement of the thickness of nanopapers

The thickness of nanopapers was measured by using a micrometer (Lorentzen and Wettre, precision 1 μm). Each nanopaper was measured at least five different locations, which should be evenly distributed on the whole nanopaper. The mean value was used in the calculations to determine the mechanical test measurement.

2.4.2. Polarized light microscopy

An Olympus BH-2 optical microscope with 10 × objective lens was used to observe the iridescence in the nanopapers with the assistance of two polarized light filters. Samples were viewed under white light conditions.

2.4.3. Morphological investigation

The shape and size of the obtained CNWs and CNFs suspensions were analyzed by a transmission electron microscope (TEM, JEOL JEM-100CX, Japan) at 80 kV. Drops of dilute suspensions were deposited onto glow-discharged, carbon-coated electron microscopy grids; excess liquid was absorbed by a piece of filter paper. Furthermore, the nanopapers were fractured in liquid nitrogen to expose the middle part of cross sections for SEM observations by fixed on a metal stub using carbon tape and coated with gold.

2.4.4. UV-vis transmittance measurements

The optical transmittances of the films were measured from 350 to 900 nm using a Shimadzu UVmini-1240 spectrophotometer and were correlated based on the nanopaper thicknesses using the Lambert–Beer's law.

2.4.5. Wide-angle X-ray diffractions (XRD) analysis

Wide-Angle X-ray Diffractions were carried out by a Philips X'Pert X-diffractometer with Cu-Kα radiation operating at $\lambda = 0.1540$ nm (40 kV, 40 mA). Data were obtained in a 2θ scale from 5 to 50°.

The degree of crystallinity could be relatively expressed by the percentage crystallinity index (% CrI). (Habibi, Chanzy, & Vignon, 2006) The equation used to calculate the CrI was described by Segal et al. (Segal, Creely, Martin, & Comrad, 1959) as follows:

$$CrI(\%) = [(I_{002} - I_{am})/I_{002}] \times 100$$

where I_{002} is the counter reading at peak intensity at a 2θ angle close to 22° representing the crystalline part and I_{am} is the counter reading at peak intensity at 2θ close to 18° representing the amorphous part in cellulose.

2.4.6. Thermal Analysis

Thermal gravimetric analysis (TGA) was performed by using a TA-2000 analyzer (TA Instrument) under nitrogen purge with a flow rate of 100 mL/min. The scanning rate was 10 °C/min and the temperature range was from 40 to 600 °C.

2.4.7. Tensile strength tests

The tensile strength of the nanopapers was measured with a tensile testing machine (Instron 5567 Universal Testing Machine) fitted with a 100 N load cell at a crosshead speed of 1 mm/min. The samples were cut in the rectangular specimens with a width of 12 mm and length of 35 mm. The measurements were performed at 23 °C and relative humidity of 50%.

2.4.8. Water contact angel (WCA) measurements

The WCA was measured by a DSA 100 drop shape analysis system (Kruss Gmbh). The volume of the water droplet for each measurement was kept at 3×10^{-9} m^3.

3. Results and discussion

3.1. Polarized light microscopy

Fig. 1 shows the images of nanopaper-0 (Fig. 1a), nanopaper-1 (Fig. 1b), nanopaper-5 (Fig. 1c), and nanopaper-10 (Fig. 1d) observed in transmission between crossed polars in an optical microscope. Both nanopaper-0 and nanopaper-1 show remarkable iridescence and usual multidomain structure, which indicates the existence of chiral nematic structures in these nanopapers. However, it can be obviously observed that the color of nanopaper-5 in

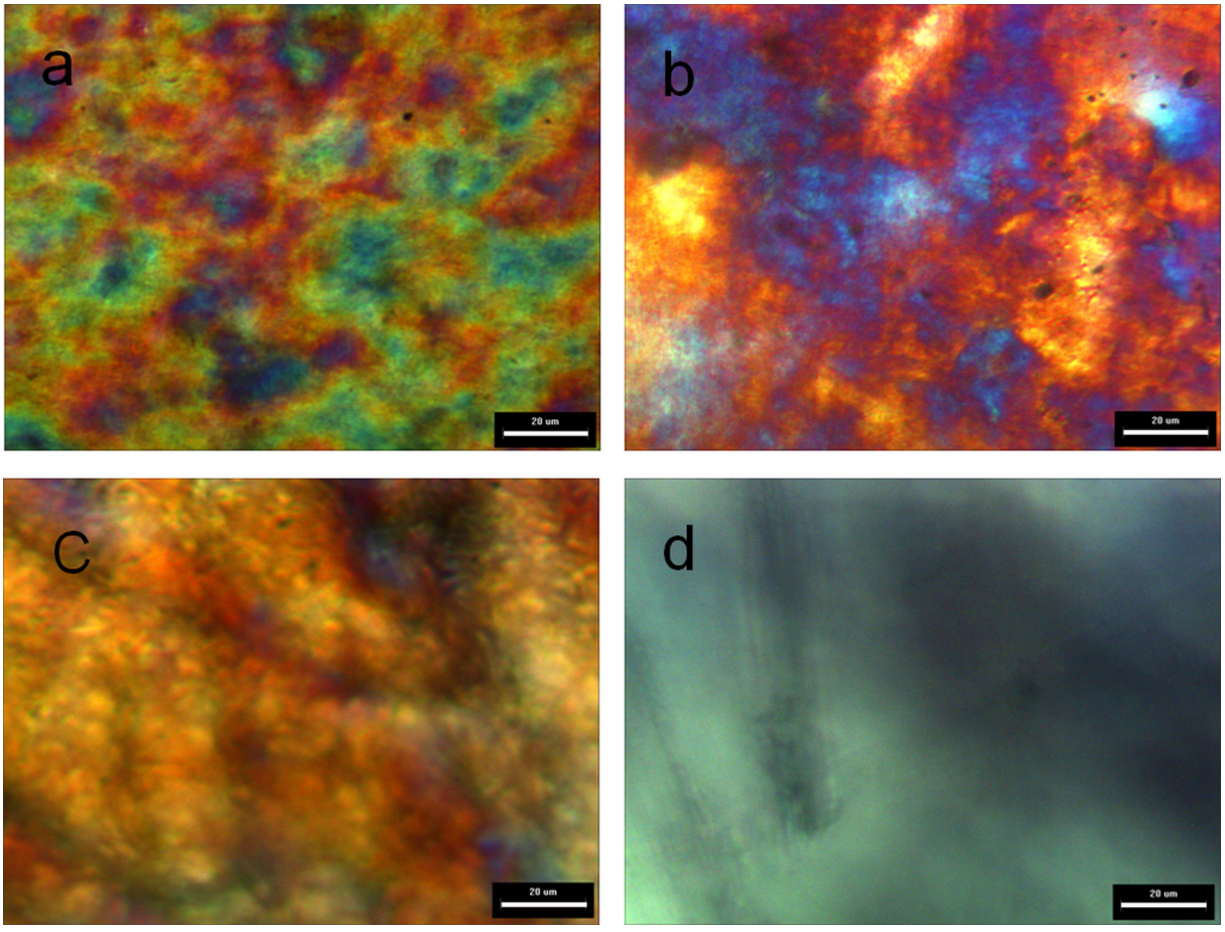

Fig. 1. The images of nanopaper-0 (a), nanopaper-1 (b), nanopaper-5 (c) and nanopaper-10 (d) observed in transmission between crossed polars using an optical microscope (scale bar = 20 μm).

Fig. 1c became monotonous and dim. The iridescence of nanopaper is even faded out (in Fig. 1d) when the content of CNFs increased to 10 wt%, suggesting the disappearance of liquid crystal structure in the nanopaper. These results indicate that the liquid crystal structure of CNWs can be maintained under the addition of low amount of CNFs. However, the excessive introduction of CNFs will block the formation of liquid crystal structure of CNWs-based nanopaper.

3.2. TEM and SEM analysis

The morphology of the obtained CNWs suspension, CNFs suspension and nanocomposites films was further analyzed by TEM and SEM and shown in Fig. 2. Fig. 2a shows the TEM image of the CNWs suspension, which has been isolated from commercial cotton by acid hydrolysis. It can be observed that the CNWs suspension consists of rod-like crystalline celluloses with 10–20 nm in diameter and 150–200 nm in length. Their aspect ratios are around 10–20. The CNWs suspension has a good stability because sulfate groups were grafted onto the surface of CNWs during acid hydrolysis, which created a strong electrostatic repulsion between the anionic sulfate ester groups at the surface (Xiong et al., 2012). The TEM morphology of the obtained CNFs is shown in Fig. 2b, which appears as an inter-connected web structure. The diameter of CNFs is 20 ± 10 nm while the nanofiber length is estimated more than 1000 nm, which leads to a higher aspect ratio than CNWs.

Fig. 2(c–f) shows the cross section of the nanocomposite films reinforced by CNFs. With the increase of CNFs content, it can be observed that the cross section of the nanopapers have become more dense. This might be ascribed to the fact that the CNFs are considered to form hydrogen bonds with CNWs, which can remarkably enhance the mechanical properties of the CNWs-based nanopaper. However, in these nanopapers, it is difficult to identify the CNFs because CNWs and CNFs have similar diameter and most of CNFs were embedded in the CNWs matrix due to the strong interactions between them. In Fig. 2(c and d), the twisted helical organized layer structure can be observed in the nanopaper-0 and nanopaper-1 (as indicated by red circles in Fig. 2c and Fig. 2d), indicating the preservation of chiral nematic structure in the nanopapers. When the CNFs content reaches 10 wt%, however, twisted helical organized layer structure is difficult to be detected. This result is well consistent with the polarized light microscopy analysis.

3.3. UV-vis transmittance measurements

Fig. 3 shows the UV-vis transmittance of approximately 50 μm thick nanopaper-0, nanopaper-1, nanopaper-5, and nanopaper-10. The transmittance at 900 nm is about 53% for the nanopaper-0, while it is about 75%, 77%, and 71% for the nanopaper-1, nanopaper-5, and nanopaper-10, respectively. Recently, Fukuzumi et al.(Fukuzumi, Saito, Iwata, Kumamoto, & Isogai, 2009) reported light transmittance as high as 90% through 20-μm films prepared from TEMPO-oxidized cellulose nanofibers. However, in their

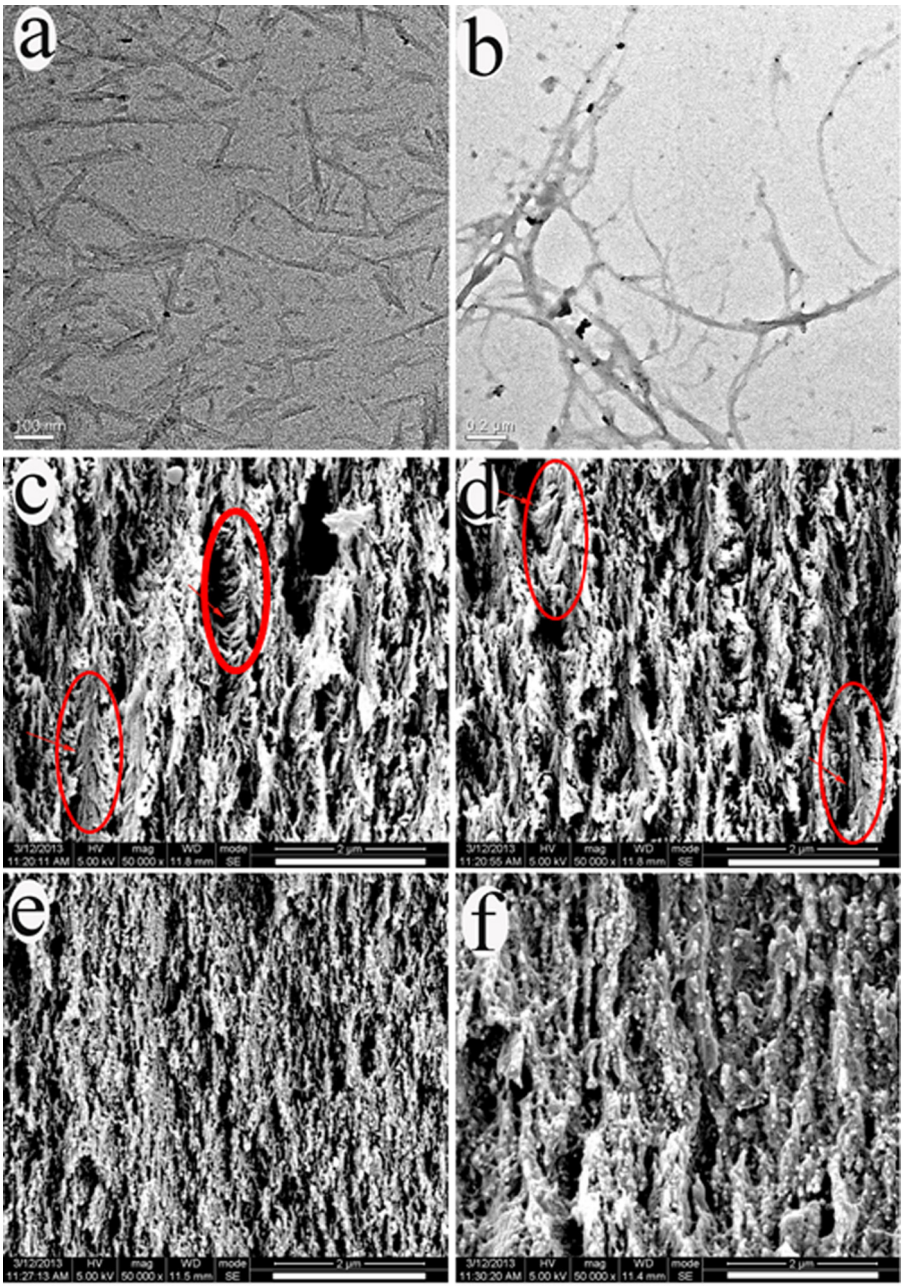

Fig. 2. TEM images of CNWs (a) and CNFs (b); SEM images of nanopaper-0 (c), nanopaper-1 (d), nanopaper-5 (e) and nanopaper-10 (f).

study, un-fibrillated and partly fibrillated fibers were removed from the gel by filtration through a nylon cloth with 20-μm pores. According to Nogi et al. (Nogi, Lwamoto, Nakagaito, & Yano, 2009), if the CNFs are densely packed and the interstices between the fibers are small enough to avoid light scattering, the cellulosic material becomes transparent. As discussed in the SEM analysis, the introduction of CNFs in CNWs resulted in a more dense structure of the prepared nanocomposites. Therefore, the introduction of CNFs would lead to the higher light transmittance of CNWs-based nanopaper. However, compared with nanopaper-1 and nanopaper-5, the nanopaper-10 has a slightly lower transparency, which might result from the existence of some cellulose fibers with large size in the CNFs. The appearance of the prepared nanopaper-0 and nanopaper-1 is shown in the inserted image in Fig. 3. It can be observed that visual transparency was indeed significantly improved with the introduction of CNFs.

3.4. XRD analysis

XRD analysis was carried out to examine the changes in the crystalline structure of the nanocomposites. Fig. 4 shows the XRD patterns of the obtained nanopaper-0 and nanopaper-1. Three main peaks at $2\theta = 14.9^\circ$, 16.5° and 22.6° can be observed in both films, which correspond to the cellulose I crystals where the parallel chains are strongly intermolecularly hydrogen bonded (Walther, Timonen, Diez, Laukkanen, & Ikkala, 2011). It suggested that the original crystalline structure of native cellulose fibers was essentially maintained in the CNWs and CNFs. Moreover, the CrI of both samples was also calculated, and the CrI is decreased from 91.5 for nanopaper-0 to 90 for nanopaper-1. The decrease of the CrI was undoubtedly associated with the addition of CNFs, which has a lower degree of crystallinity than CNWs. On the other hand, the existence of CNFs would improve the limited

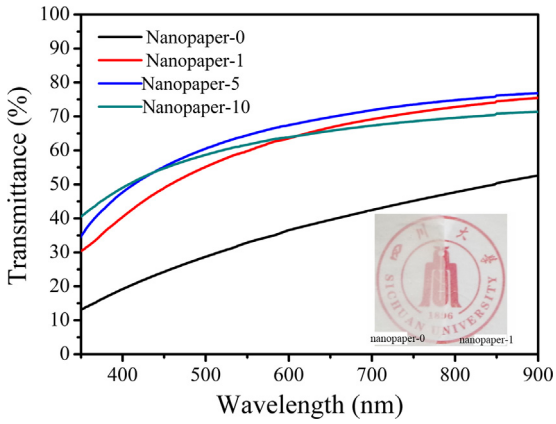

Fig. 3. UV-vis transmittance of approximately 50 μm thick nanopaper-0, nanopaper-, nanopaper-5, and nanopaper-10, the inserted image shows the photograph of nanopaper-0 and nanopaper-1 on the logo of Sichuan University.

flexibility of CNWs film, because the CNFs contain a lot of amorphous regions.

3.5. Thermal analysis

Considering the importance of thermal stability of cellulose-based materials in many applications, we examined the thermal decomposition behaviors of cellulose nanopapers by TGA analysis in nitrogen atmosphere. As a result of their different chemical structures, CNWs and CNFs usually decompose at different temperatures. Fig. 5 shows the typical TGA curves of CNWs nanopaper with different contents of CNFs. For all the samples, the 1st stage weight loss occurred at below 150 °C. This approximate 4% weight loss apparently resulted from the evaporation of adsorbed water. The 2nd stage of weight loss which occurred at around 200–300 °C could be attributed to the depolymerization of cellulose (Jonoobi, Khazaeian, Tahir, Azry, & Oksman, 2011; Roman & Winter, 2004). The degradation temperature of the films was found to follow the order: nanopaper-10 > nanopaper-5 > nanopaper-1 > nanopaper-0. This result indicates that the existence of CNFs can improve the thermal stability of CNWs. Although CNWs has a higher degree of crystallinity than CNFs because of the remove of amorphous region, the thermal stability of CNWs is poorer than that of CNFs. This is because the sulfate groups introduced on cellulose chains catalyzed the thermal degradation of cellulose. According to Roman et al. (Roman & Winter, 2004), the catalysis could proceed either directly through the acid molecules or indirectly by promoting dehydration reactions.

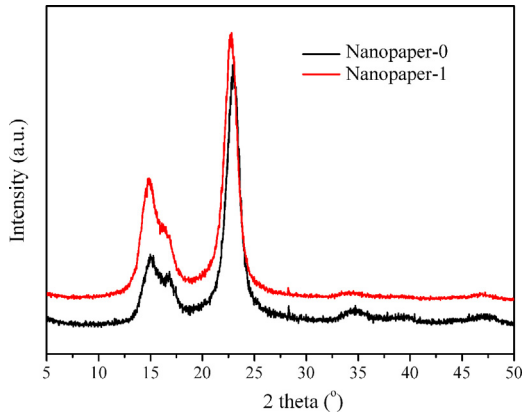

Fig. 4. XRD patterns of the obtained nanopaper-0 and nanopaper-1.

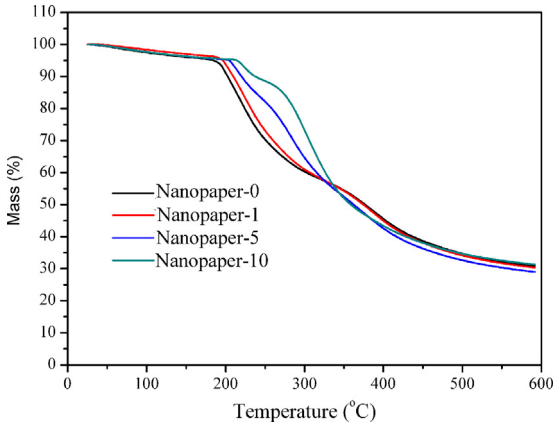

Fig. 5. TGA curves of nanopaper-0 (a), nanopaper-1 (b), nanopaper-5 (c) and nanopaper-10 (d).

3.6. Mechanical properties

Fig. 6a shows the typical stress–strain curves of nanopaper-0, nanopaper-1, nanopaper-5, and nanopaper-10. The effect of CNFs content on the mechanical properties of CNWs nanopaper is investigated. The average values of tensile strength, Young's modulus and elongation at break of the as-prepared films are shown in Table 1. It can be observed that the neat CNWs nanopaper is very weak, which is indicated by the maximum tensile strength of 14.25 MPa. However, the incorporation of CNFs could result in a significant improvement in the tensile strength of the nanocomposite nanopapers. With addition of 1 wt% CNFs, the tensile strength of CNWs nanopaper was increased by 76%, indicating the high load bearing capacity of CNFs. Moreover, with the increase of CNFs content from 1 wt% to 10 wt%, the tensile strength of CNWs nanopaper is 37.46 MPa, improved by 114% compared with that of neat CNWs-based nanopaper. Besides, the Young's modulus of nanopaper is always improved with the presence of CNFs. These results agree well with other reports (Svagan, Samir, & Berglund, 2007; Peng, Ren, Zhong, & Sun, 2011). Fig. 6(b and c) shows the photographs of nanopaper-0 and nanopaper-1 to investigate the effect of CNFs on bending strength of the CNWs nanopapers. As we all know, the neat CNWs-based nanopaper is very brittle due to its rigid rod-like structures instead of amorphous regions. As shown in Fig. 6b, the nanopaper-0 was broken into two pieces by bending gently. However, only adding 1 wt% CNFs into the CNWs nanopaper, it can be bended repeatedly for a large angle without any ruptures as shown in Fig. 6c. This character of bending strength also can be proven by the decrease of Young's modulus and increase of elongation at break as shown in Table 1. Furthermore, similar results were also reported for other nanopapers reinforced with CNFs. The tensile strength of amylopectin film increased from 0.35 to 15.0 MPa by incorporation of 20 wt% CNFs into the film (Svagan et al., 2007). High-performance nanocomposite films based on polyvinyl alcohol and CNFs could be obtained from their mixture. The nanocomposite film showed an increase in tensile strength from 65 (pure polyvinyl alcohol film) to 103 MPa (composite film with 5 wt% CNFs) (Wang & Sain, 2007).

Table 1
Mechanical properties of nanopaper-0, nanopaper-1, nanopaper-5, and nanopaper-10.

Samples	Tensile strength (MPa)	Elongation at break (%)	Young's modulus (MPa)
Nanopaper-0	14.25	0.466	3417
Nanopaper-1	25.88	1.24	4423
Nanopaper-5	33.25	1.27	4336
Nanopaper-10	37.46	1.43	3768

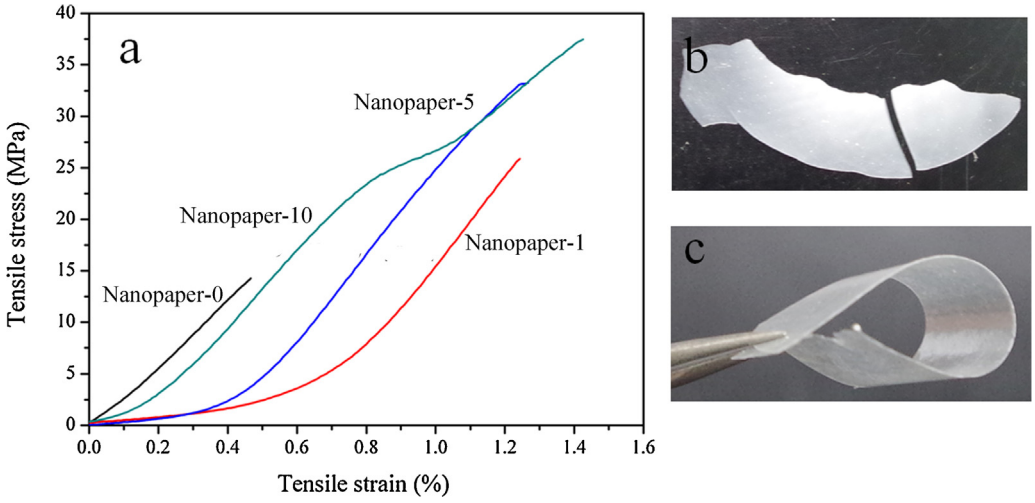

Fig. 6. Stress–strain curves of nanopaper-0, nanopaper-1, nanopaper-5, and nanopaper-10 (a), the photographs of fragile nanopaper-0 (b) and flexible nanopaper-1 (c).

Xylan-rich hemicelluloses nanocomposites reinforced with CNFs also showed improved mechanical properties (Peng et al., 2011).

The rigid rod-like structure and the short length of CNWs would result in the brittle character of CNWs-based material. On the other hand, the significant enhancement of tensile strength of the CNWs nanopaper with the addition of CNFs could be ascribed to the high aspect ratio of CNFs as well as the strong interactions between CNFs and CNWs matrix. The interaction between the matrix and reinforcement plays a critical role in determining the external load transfer within the nanopapers. The strong interactions (Van der

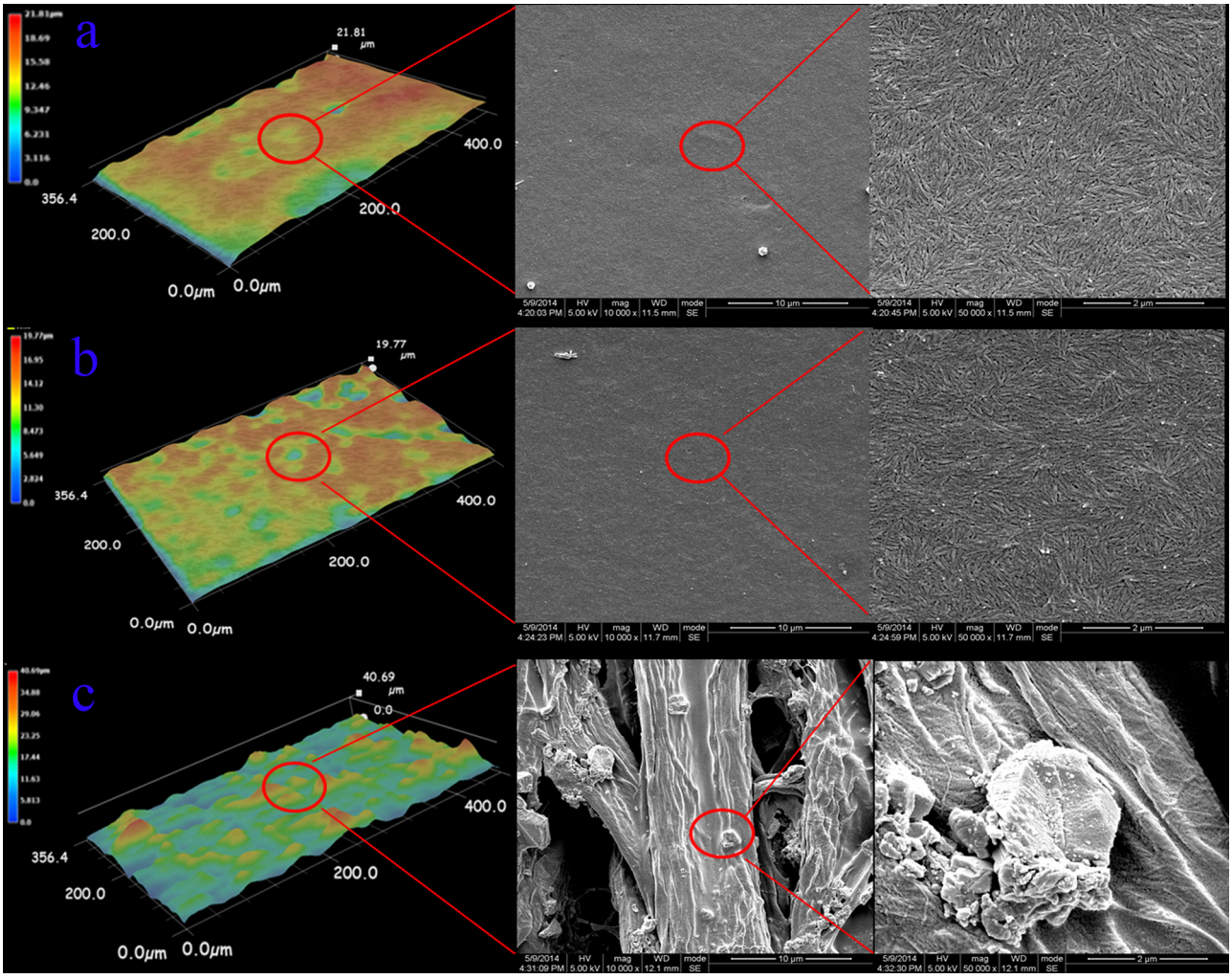

Fig. 7. 3D surface topography and surface SEM images of nanopaper-0 (a), nanopaper-1(b) and commercial paper (c).

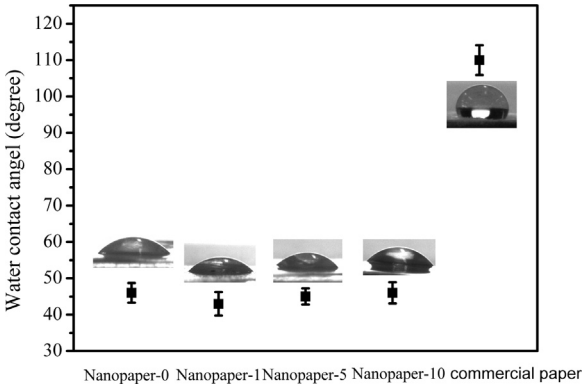

Fig. 8. Water angel contact of nanopaper-0, nanopaper-1, nanopaper-5, nanopaper-10, and commercial paper.

Waals forces and strong hydrogen bonding) between CNFs and CNWs were resulted from their nanosize-effect and same molecular structure, which allow good interfacial adhesion between CNWs matrix and the reinforcement (CNFs). Moreover, the strong interactions between CNWs and CNFs were used to develop molecular anchors, which give new chemical functions to cellulose crystals (Huber et al., 2012). Therefore, external load can be effectively transferred between matrix (CNWs) and CNFs, which results in the reduction in stress concentration and crack formation within the nanopapers. These results suggest the possibility of manufacturing CNWs-based nanopapers with high mechanical performance.

3.7. Surface roughness

In order to evaluate the surface roughness of the nanopaper, we have carried out the 3D surface topography images, surface SEM analysis and water contact angle. The 3D surface topography images of nanopaper-0, nanopaper-1, and commercial paper are shown in Fig. 7. The maximum surface protrusion (MSP) values of the nanopaper-0 and nanopaper-1 are around 20 μm, while that of commercial paper is about 40 μm. Besides, we can observe from the 3D images that the nanopaper has less protrusion than commercial paper, which indicates the nanopaper has much lower surface roughness.

SEM was further employed to observe the surface roughness of the nanopaper. It can be seen from Fig. 7 that CNWs are evenly dispersed on the surface of the nanopaper. However, it is hard to distinguish CNFs from CNWs, because they have similar diameter and most of CNFs are embed in the matrix. In addition, like the typical cellulose nanopapers, small pores can still be observed in the image. It can be clearly seen that nanopaper-0 and nanopaper-1 have similar surface structure. However, the surface of commercial paper consists of cellulose fiber with large sizes, which resulted in a great number of large porosities in the surface. As a result, the commercial paper has a much higher surface toughness.

It was widely reported that the surface roughness of the substrate plays an important role in the wettability of the surface. Therefore, water contact angle (WCA) measurements were carried out to estimate wettability. According to the previous report (Ryan & Poduska, 2008), it was observed that the rough surfaces may have substantially larger contact angles due to heterogeneous wetting. For example, a droplet will not entirely wet the rough surface and may leave pockets of air between the droplet and the substrate (Cassie & Baxter, 1944). As shown in Fig. 8, we can see that the WCAs of all nanopapers are essentially the same, which indicates the similar surface roughness of these samples. However, due to its high surface roughness, the WCA of commercial paper is round 110 °C. The WCA results are well in agreement with the 3D surface topography images and surface SEM analysis.

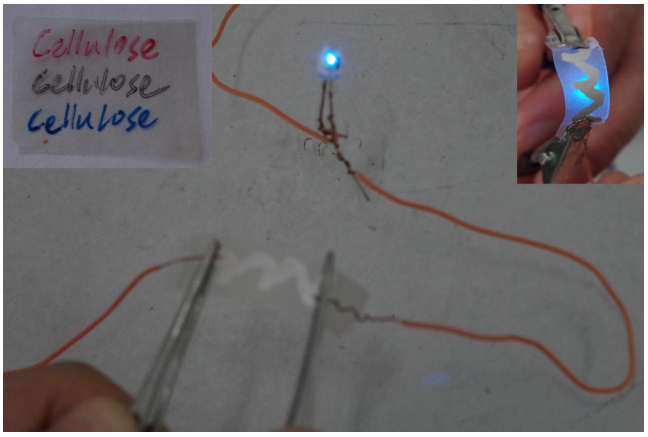

Fig. 9. Image of the highly transparent, writable, flexible, and conductive hybrid paper lighting up an LED device; the inset (right) shows LED placed under the nanopaper; the insert (left) is the words written on the nanopaper using different color pen.

3.8. Writable surface

To evaluate whether our transparent hybrid nanopaper preserves these properties like commercial paper, we evaluated its writability using an aqueous silver ink. The word“NCC” is drawn on the surface of the hybrid paper using a pen saturated with aqueous silvers ink and dried under ambient conditions. Then, a green LED light is connected with the curved conductive hybrid nanopaper using a metal line to form a conductive network (Fig. 9, LED was placed under the nanopaper in the inserted image). The lighting LED is illuminated by using two 1.5 V batteries. Additionally, we also have used three other color pens to write on this nanopaper to test its writability. As shown in the inserted image in Fig. 9, it is very easy to write“cellulose” on the nanopaper like a commercial cellulose paper. The results indicated that the writable, flexible and transparent properties of the hybrid nanopaper may have the potential to fabricate “writable electronics.”

4. Conclusion

In this paper, a facile and environmentally friendly process was developed to produce flexible and iridescent all-cellulose films by introducing CNFs into CNWs matrix. The process was carried out at room temperature and does not rely on harmful solvents. With incorporation of only 1 wt% CNFs, the tensile strength of CNWs-based film was increased by 76% and it can be bended repeatedly for a large angle without any ruptures. Furthermore, the nanocomposite film also exhibited remarkable iridescence, improved transparence and enhanced thermal stability. The biocomposite film consisting of biodegradable CNFs and CNWs is fully biodegradable, which renders them advantageous in terms of environmental protection.

Acknowledgments

The authors would like to thank the National Science Foundation of China (51203105) for financial support.

References

Beck, S., Bouchard, J., & Berry, R. (2011). Controlling the reflection wavelength of iridescent solid films of nanocrystalline cellulose. *Biomacromolecules*, *12*, 167–172.

Cassie, A., & Baxter, S. (1944). Wettability of porous surfaces. *Transactions of the Faraday Society*, *40*, 546–551.
Chen, W., Yu, H., Li, Q., Liu, Y., & Li, J. (2011). Ultralight and highly flexible aerogels with long cellulose I nanofibers. *Soft Matter*, *7*, 10360–10368.
Chen, W., Yu, H., Liu, Y., Chen, P., Zhang, M., & Hai, Y. (2011). Individualization of cellulose nanofibers from wood using high-intensity ultrasonication combined with chemical pretreatments. *Carbohydrate Polymers*, *83*, 1804–1811.
Chen, W., Yu, H., & Liu, Y. (2011). Preparation of millimeter-long cellulose I nanofibers with diameters of 30-80 nm from bamboo fibers. *Carbohydrate Polymers*, *86*, 453–461.
Fang, Z., Zhu, H., Preston, C., Han, X., Li, Y., Lee, S., et al. (2013). Highly transparent and writable wood all-cellulose hybrid nanostructured paper. *Journal of Materials Chemistry C*, *1*, 6191–6197.
Fukuzumi, H., Saito, T., Iwata, T., Kumamoto, Y., & Isogai, A. (2009). Transparent and high gas barrier films of cellulose nanofibers prepared by TEMPO-Mediated oxidation. *Biomacromolecules*, *10*, 162–165.
Guo, B., Chen, W., & Yan, L. (2013). Preparation of flexible, highly transparent, cross-linked cellulose Thin film with high mechanical strength and low coefficient of thermal expansion. *ACS Sustainable Chemistry & Engineering*, *1*, 1474–1479.
Gao, K., Shao, Z., Wu, X., Wang, X., Li, J., Zhang, Y., et al. (2013). Cellulose nanofibers/reduced graphene oxide flexible transparentconductive paper. *Carbohydrate Polymers*, *97*, 243–251.
Habibi, Y., Chanzy, H., & Vignon, M. R. (2006). TEMPO-mediated surface oxidation of cellulose whiskers. *Cellulose*, *13*, 679–687.
Huber, T., Müssig, J., Curnow, O., Pang, S., Bickerton, S., & Staiger, M. P. (2012). A critical review of all-cellulose composites. *Journal of Materials Science*, *47*, 1171–1186.
Hu, L., & Cui, Y. (2012). Energy and environmental nanotechnology in conductive paper and textiles. *Energy and Environmental Science*, *5*, 6423–6435.
Hu, L., Liu, N., Eskilssond, M., Zheng, G., McDonougha, J., Wågberg, L., et al. (2013). Silicon-conductive nanopaper for Li-ion batteries. *Nano Energy*, *2*, 138–145.
Jonoobi, M., Khazaeian, A., Tahir, P. M., Azry, S. S., & Oksman, K. (2011). Characteristics of cellulose nanofibers isolated from rub-berwood and empty fruit bunches of oil palm using chemo-mechanical process. *Cellulose*, *18*, 1085–1095.
Jung, R., Kim, H., Kim, Y., Kwon, S., Lee, H. S., & Jin, H. (2008). Electrically conductive transparent papers using multiwalled carbon nanotubes. *Journal of Polymer Science Part B: Polymer Physics*, *46*, 1235–1242.
Klemm, D., Kramer, F., Moritz, S., Lindstrom, T., Ankerfors, M., Gray, D., et al. (2011). Nanocelluloses: A new family of nature-based materials. *Angewandte Chemie-Iinternational Eedition*, *50*, 5438–5466.
Li, Y., Zhu, H., Gu, H., Dai, H., Fang, Z., Weadock, Z. J., et al. (2013). Strong transparent magnetic nanopaper prepared by immobilization of Fe_3O_4 nanoparticles in a nanofibrillated cellulose network. *Journal of Materials Chemistry A*, *1*, 15278–15283.
Ma, H., Zhou, B., Li, H., Li, Y., & Ou, S. (2011). Green composite films composed of nanocrystalline cellulose and a cellulose matrix regenerated from functionalized ionic liquid solution. *Carbohydrate Polymers*, *84*, 383–389.
Madaria, A. R., Kumar, A., & Zhou, C. (2011). Large scale, highly conductive and patterned transparent films of silver nanowires on arbitrary substrates and their application in touch screens. *Nanotechnology*, *22*, 245201.
Nogi, M., Lwamoto, S., Nakagaito, A. N., & Yano, H. (2009). Optically transparent nanofiber paper. *Advanced Materials*, *21*, 1595–1598.
Nyholm, L., Nyström, G., Mihranyan, A., & Strømme, M. (2011). Toward flexible polymer and paper-based energy storage devices. *Advanced Materials*, *23*, 3751–3769.
Peng, X., Ren, J., Zhong, L., & Sun, R. (2011). Nanocomposite films based on xylan-rich hemicelluloses and cellulose nanofibers with enhanced mechanical properties. *Biomacromolecules*, *12*, 3321–3329.
Roman, M., & Winter, W. T. (2004). Effect of sulfate groups from sulfuric acid hydrolysis on the thermal degradation behavior of bacterial cellulose. *Biomacromolecules*, *5*, 1671–1677.
Russo, A., Ahn, B. Y., Adams, J. J., Duoss, E. B., Bernhard, J. T., & Lewis, J. A. (2011). Pen-on-paper flexible electronics. *Advanced Materials*, *23*, 3426–3430.
Ryan, B., & Poduska, K. (2008). Roughness effects on contact angle measurements. *American Journal of Physics*, *76*, 1074–1077.
Segal, L., Creely, J. J., Martin, A. E., Jr., & Comrad, C. M. (1959). An empirical method for estimating the degree of crystallinity of native cellulose using the X-ray diffractometer. *Textile Research Journal*, *29*, 786–794.
Svagan, A. J., Samir, M. A. S. A., & Berglund, L. A. (2007). Biomimetic polysaccharide nanocomposites of high cellulose content and high toughness. *Biomacromolecules*, *8*, 2556–2563.
Walther, A., Timonen, J., Diez, I., Laukkanen, A., & Ikkala, O. (2011). Multifunctional high-performance biofibers based on wet-extrusion of renewable native cellulose nanofibrils. *Advanced Materials*, *23*, 2924–2928.
Wang, B., & Sain, M. (2007). Isolation of nanofibers from soybean source and their reinforcing capability on synthetic polymers. *Composite Science and Technology*, *67*, 2521–2527.
Xiong, R., Zhang, X., Tian, D., Zhou, Z., & Lu, C. (2012). Comparing microcrystalline with spherical nanocrystalline cellulose from waste cotton fabrics. *Cellulose*, *4*, 1189–1198.
Zhang, W., Zhang, X., Lu, C., Wang, Y., & Deng, Y. (2012). Flexible and transparent paper-based ionic diode fabricated from oppositely charged microfibrillated cellulose. *Journal of Physical Chemistry C*, *116*, 9227–9234.
Zhu, H., Parvinian, S., Preston, C., Vaaland, O., Ruan, Z., & Hu, L. (2013). Transparent nanopaper with tailored optical properties. *Nanoscale*, *5*, 3787–3792.